Actively mode-locked all-fiber laser by 5 MHz transmittance modulation of an acousto-optic tunable bandpass filter

M Bello-Jiménez[1], E Hernández-Escobar[1], A Camarillo-Avilés[1], O Pottiez[2], A Díez[3] and M V Andrés[3]

[1]Instituto de Investigación en Comunicación Óptica (IICO), Universidad Autónoma de San Luis Potosí, Av. Karakorum No. 1470 Lomas 4ª Secc., 78210 San Luis Potosí, México
[2]Centro de Investigaciones en Óptica (CIO), Loma del Bosque No. 115, Col. Lomas del Campestre, León, Guanajuato 37150, México
[3]Universidad de Valencia, Departamento de Física Aplicada y Electromagnetismo, ICMUV, c/Dr. Moliner 50, Burjassot, 46100 Valencia, Spain

E-mail: miguel.bello@uaslp.mx

Abstract. Active mode-locking of an all-fiber ring laser by transmittance modulation of an in-fiber acousto-optic tunable bandpass filter (AOTBF) is reported. Cavity loss modulation is achieved by full acousto-optic mode re-coupling cycle induced by standing flexural acoustic waves. The modulator permits the implementation of 28 dB of nonresonant light suppression, 1.4 nm of modulation bandwidth, 74 % of modulation depth and 4.11 dB of optical loss in a 72.5 cm-long all-fiber configuration. The effects of the modulated AOTBF on the laser performance are investigated. Transform-limited optical pulses of 8.8 ps temporal width and 6.0 W peak power were obtained at 4.87 MHz repetition rate.

Keywords: Mode-locked fiber lasers, Acousto-optic modulation, Fiber optics.

1. Introduction

Ultrashort optical pulses with temporal widths from a few picoseconds to several hundreds of femtoseconds have become essential for a large variety of applications. Examples of these applications can be found in optical communications, biomedical research, spectroscopy and material processing, among others [1–2]. In many of these applications the quality of the pulse is an important factor, and the generation of clean ultrashort optical pulses has attracted the attention of researchers for a relatively long time. For applications in the ultrashort pulse regime, passive mode locking is the preferable technique, but sometimes the generation of low-intensity radiation and the limited repetition rate becomes its major shortcoming. Conversely, active mode locking allows a tight control over intracavity parameters, such as the cavity losses or the round-trip phase change, enabling improvements on the output pulse characteristics. Therefore, active mode locking is the preferred technique in many practical applications. Nevertheless, a detrimental factor of this technique is the relatively long pulse duration as a result of the limited optical bandwidth of the active mode locker.

In the framework of actively mode-locked lasers, many researchers have proposed and demonstrated different configurations to produce high-quality ultrashort optical pulses [3–9]. Among them, all-fiber arrangements are very attractive devices since they can reduce intracavity losses associated with bulk components and can be designed to adjust cavity dispersion simply by the inclusion of optical fibers with different group velocity dispersions. In addition to these benefits, all-fiber arrangements provide high stability, large optical-damage threshold and low maintenance requirements.

One of the most common configurations of actively mode-locked fiber lasers relies on the use of spectral filters to prevent laser emission at different wavelengths of the gain medium. Examples of these schemes can be found in [7–14], where active mode locking by using electro-optic modulators [7,8], in-fiber

amplitude acousto-optic (AO) modulators [9–11], AO superlattice modulators [12,13] and conventional AO tunable filters [14] is reported. Therefore, a common shortcoming is the restriction of wavelength emission and the limited optical bandwidth. This condition has motivated the improvement of active mode lockers to eliminate the inclusion of filtering devices in the laser cavity. In this regard, in-fiber AO devices can be designed to realize a bandpass operation with a widely tunable spectral response [5,15–17]. In previous publications we have reported the operation of an efficient in-fiber AO tunable bandpass filter (AOTBF) that combines the dynamical properties of flexural acoustic waves together with a core mode blocker (CMB) composed of a tiny section of coreless optical fiber [16,17]. Now, with the objective of expanding the application of the AOTBF to perform active mode locking, acoustic reflection is intentionally induced. In this way, a standing flexural acoustic wave is generated and the transmission of the AOTBF can be modulated, while preserving the tunable bandpass characteristics. The device demonstrates amplitude modulation at two times the acoustic frequency used, a high modulation depth, moderate insertion loss, and good modulation bandwidth.

In this paper our purpose is to show the performances of an actively mode-locked source by implementing this novel type of amplitude modulated AOTBF. The proposed scheme presents the following advantages: (i) high rejection efficiency of 28 dB, this value is at least 10 dB in depth greater than conventional all-fiber AO attenuators [18–20], (ii) intrinsic spectral filtering (linewidth ~1 nm), that prevents laser emission at unwanted wavelengths and can be tuned over a broad wavelength range, (iii) simplicity in fabrication, the mode locker does not require complicated procedures for the CMB and avoids the inclusion of specialty optical fibers, (iv) being an all-fiber device, it can handle high power. However, the main disadvantage that could be associated with the present scheme is a relatively long interaction length (~70 cm). In this respect, it is worth noting that some characteristics of the present device, such as interaction length and modulation bandwidth, could be further improved, as will be discussed in the next sections.

2. The acousto-optic bandpass modulator

A schematic of the acousto-optic tunable bandpass modulator is depicted in figure 1. The AO device relies on a core mode blocker (CMB) composed of a 1.185-mm long coreless optical fiber (Thorlabs FG125LA) spliced between two sections of single-mode optical fibers (SMF-28) with lengths L_1 and L_2, respectively. The acousto-optic bandpass modulator (AOBM) consists of a radio frequency (RF) source, a piezoelectric disk (PD) and an aluminum concentrator horn. The horn focuses the vibrations into the fiber through its tip, which is glued to an uncoated optical fiber to prevent the attenuation of the acoustic wave. In order to produce a standing flexural acoustic wave, the opposite end to the aluminum horn is firmly clamped. This produces that light transmitted at the resonant wavelength undergo an amplitude modulation at twice the frequency of the acoustic signal.
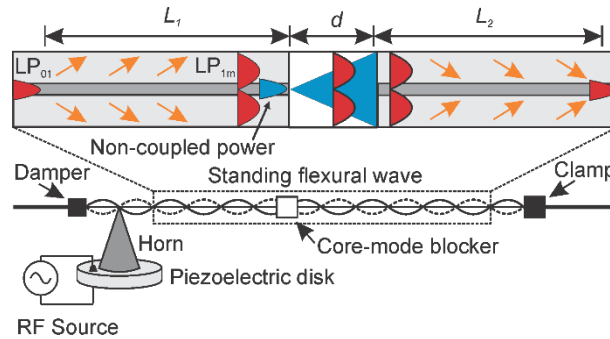

Figure 1. Experimental setup of the acousto-optic tunable bandpass modulator.

The length d of the CMB is calculated for the light leaving section L_1 to be expanded up to the outer surface at the front face of the next single-mode fiber. Considering an effective index of 1.446 for the LP_{01}

mode at 1550 nm and a refractive index of 1.444 for the coreless fiber, d is calculated as 1.185 mm. Figure 2(a) shows the transmission of the CMB in the absence of acoustic wave. This measurement was realized by illuminating the AOBM with a supercontinuum light source and detecting the transmitted signal with an optical spectrum analyzer (OSA).

This result demonstrates a strong suppression of light by at least 20 dB in a range of wavelengths between 1514 and 1600 nm, obtaining a maximum attenuation of 30 dB at 1556 nm. On the other hand, and under the effect of a traveling flexural acoustic wave, the modulator is capable to bypass the CMB via cladding propagation. Thus, the section of fiber L_1 is chosen to allow the LP_{01} mode to be coupled to a cladding mode previous the CMB, whereas the section of fiber L_2 is adjusted to find a maximum reinsertion of energy in the 1550 nm region. For the set of experiments reported here, we follow the same procedure that described in [17], L_1 was set to 24 cm in length, and the section of fiber L_2 was selected to be 48.5 cm in length, giving a total length of ~72.5 cm for the AO device. The bandpass characteristics of the modulator are depicted in figure 2(b). The strongest AO resonance, which corresponds to a LP_{01}–LP_{12} intermodal coupling, was found at the acoustic frequency (f_a) of 2.430 MHz for a voltage applied to the piezoelectric disk (V_{PD}) of 24 V (whenever we refer to voltages, it is a peak-to-peak measurement). A 3-dB optical bandwidth of 0.91 nm with minimum insertion loss of 3 dB at the resonant optical wavelength (λ_R) of 1568.8 nm is observed. The inset in figure 2(b) gives the calibration of the device, the shift of the resonant optical wavelength versus acoustic frequency. The rate of change was measured as −0.195 nm/kHz in a range from 1500 to 1600 nm.
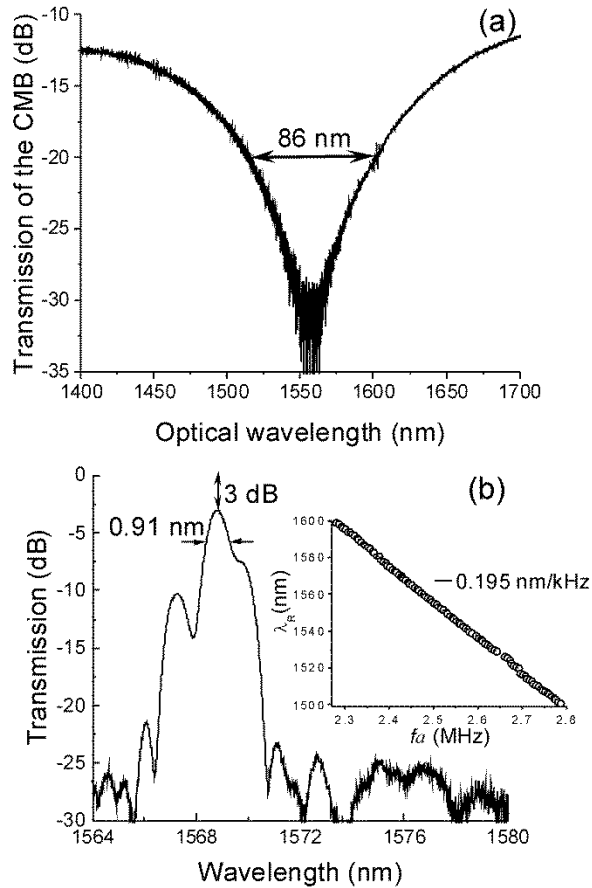

Figure 2. (a) Transmission response of the CMB in the absence of acoustic wave, (b) Maximum transfer of energy (LP_{01}–LP_{12} intermodal coupling) at the acoustic frequency of 2.430 MHz. The inset gives the calibration of the device: resonant optical wavelength vs acoustic wave frequency.

With the objective to produce a bandpass amplitude modulation, the opposite end to the aluminum horn is immersed in a drop of welding. This produces the reflection of the acoustic wave, and a standing flexural acoustic wave is generated. Under this scheme, the transmitted light oscillates in time as a result of the instantaneous coupling produced by the resulting standing wave. Hence, the transmission is amplitude modulated at two times the frequency of the acoustic wave, i. e., $f_m = 2 \times f_a$. Figure 3(a) shows the transmitted light as a function of time when a RF signal of 2.43113 MHz and 20.4 V is applied to the piezoelectric disk. The maximum modulation amplitude occurs at the resonant optical wavelength of 1569 nm. An amplitude modulation at 4.86226 MHz is clearly visible, which is two times the frequency of the piezoelectric voltage (V_{PZT}). The measurements reported in figure 3 were performed by illuminating the modulator with a tunable laser diode around the resonant optical wavelength, and detecting and monitoring the transmitted light with a standard oscilloscope. Due to the fact that the reflection coefficient is less than 1 for the acoustic wave, in addition to losses arising from acoustic attenuation, the maximum transmission is below the reference level, i.e., the transmission of the fiber when there is no acoustic wave and CMB. The maximum transmission of the device determines the insertion loss of the modulator and the difference between the maximum and minimum transmission determines the modulation depth.
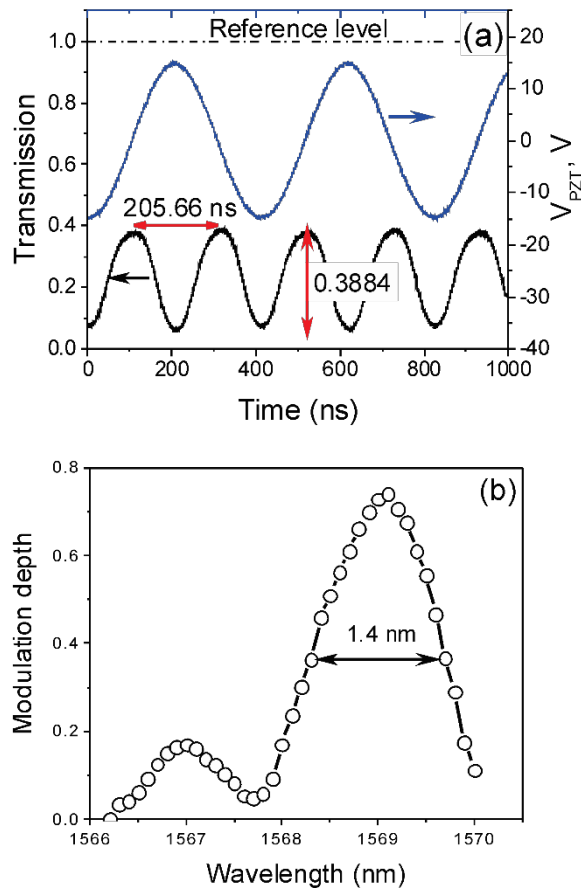

Figure 3. (a) Oscilloscope trace of the AO amplitude modulation recorded at the resonant wavelength of 1569 nm. The blue line is the RF signal of 20.4 V applied to the piezoelectric disk. (b) Modulation depth as a function of the optical wavelength at constant acoustic frequency (2.43113 MHz) and RF voltage (20.4 V).

From the results presented in figure 3(a), the measured modulation depth, defined as $(I_{max}-I_{min})/(I_{max}+I_{min})$, is 74 %, together with an insertion loss of 4.11 dB. Figure 3(b) shows the variation of modulation depth as

a function of the optical wavelength at constant acoustic frequency (2.43113 MHz) and RF voltage of 20.4 V. As it can be observed, the modulation depth decays to half of its maximum value in an optical bandwidth of 1.4 nm.

The modulation depth as a function of the RF frequency was also measured. Figure 4(a) shows the modulation depth versus the frequency detuning (Δf_a) when λ_R and V_{PD} are fixed at 1569 nm and 20.4 V, respectively. The central frequency in figure 4(a) corresponds to 2.43113 MHz, at this frequency the modulation depth is maximal, and it drops gradually to values close to 0.4 for frequency detunings of around ± 1.5 kHz and reaches a second maximum at around ± 2 kHz. For longer and shorter frequencies the transmission decays gradually to zero. From this result the acoustic frequency needs to be properly selected to achieve the maximum modulation depth at the corresponding resonant optical wavelength. Figure 4(b) shows the variation of the maximum modulation depth versus the resonant optical wavelength. This last characterization was carried out by changing the frequency and voltage of the piezoelectric disk in order to achieve the highest modulation depth at each resonant wavelength.
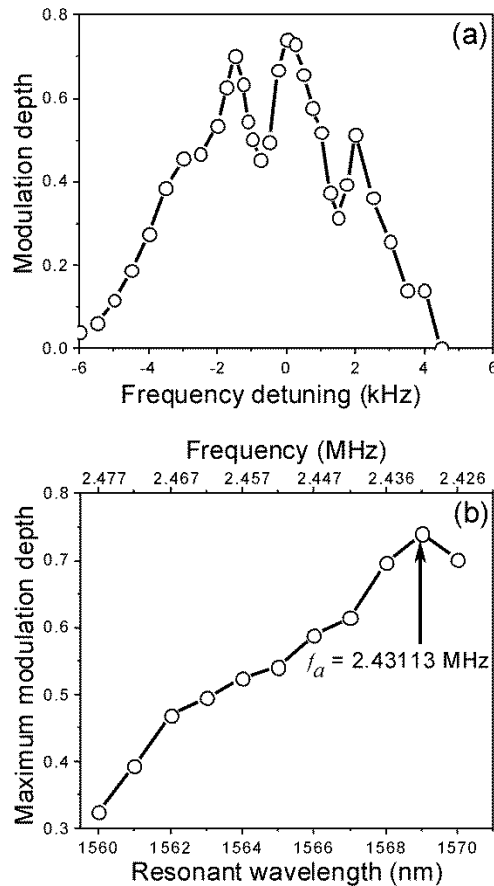

Figure 4. (a) Modulation depth as a function of the detuning frequency (Δf_a) when both the resonant wavelength (1569 nm) and the RF voltage (20.4 V) are fixed. The central acoustic frequency is 2.43113 MHz. (b) Maximum modulation depth versus resonant optical wavelength.

In the next section, the operation of the modulator as an active mode locker is demonstrated in a fiber ring laser. For an optimum performance, the AOBM could be operated with a modulation depth higher than 70 % in the optical wavelength range from 1568 to 1570 nm, which corresponds to an acoustic frequency range of 2.43669–2.42557 MHz. By using an RF voltage of around 20 V, the modulator will exhibit 4.11-dB insertion loss and 1.4-nm modulation bandwidth. Additionally, with a fine tuning of the acoustic

frequency, small error in cavity length could be compensated by matching the cavity round-trip time with the modulation period.

3. The mode-locked fiber laser

A schematic setup of the mode-locked all-fiber laser is depicted in figure 5. The gain medium is provided by a 0.8-m-long Er/Yb co-doped double-cladding fiber (CorActive, DCF-EY-10/128). The double clad fiber is pumped through a (2+1)×1 fiber combiner by a pigtailed multimode laser diode emitting at 976 nm. Then, an in-line polarization controller (PC) is included to finely tune the polarization state before the AO modulator. The modulator is connected after the PC, and is followed by a 50/50 fiber coupler. One output port of the coupler is used to provide the output light pulses, and the remaining port is connected to a delay line. This delay line was required to match the round-trip time with the modulation period. A fiber isolator is included to force unidirectional operation within the ring cavity. The cavity is closed by splicing the isolator to the signal port of the pump combiner.
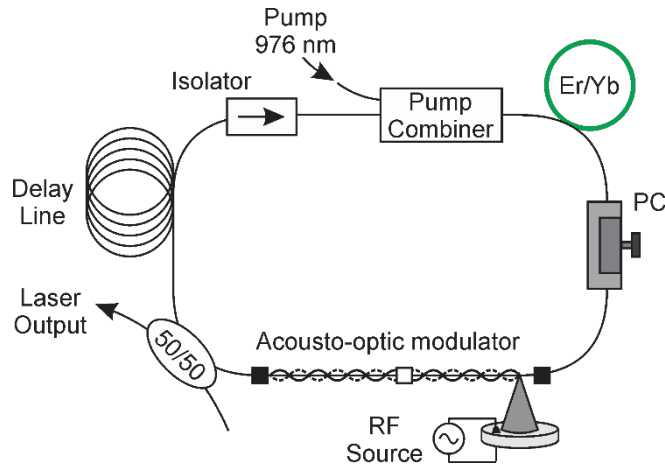

Figure 5. Schematic setup of the mode-locked fiber ring laser.

The acoustic frequency is selected to achieve the maximal modulation depth, i.e. 2.43113 MHz (see figure 3). Therefore, the frequency of modulation is 4.86226 MHz ($f_m = 2 \times f_a$). Considering an effective index (n_{eff}) of 1.446, the required cavity length, $L_{cavity} = c/(2f_a n_{eff})$, is calculated to be 42.67 m. However, small errors in cavity length are expected and these are compensated by adjusting the acoustic frequency at the rate of -1.76 cm/kHz ($\partial L_{cavity}/\partial f_a = -L_{cavity}/f_a$). Regarding cavity dispersion (D), all fiber components, with exception of the active fiber, are composed of Corning SMF-28 fiber. Thus, the cavity dispersion is anomalous.

Mode-locking operation was obtained at the pump power of 616 mW at the fundamental repetition rate of 4.869735 MHz. The train of mode-locked pulses along with the RF signal applied to the piezoelectric transducer is shown in figure 6(a). As it can be observed, the frequency of the optical pulse train is twice the frequency of the RF signal (2.434674 MHz). The measured optical spectrum of the output pulses is shown in figure 6(b). The full width at half maximum (FWHM) of the spectrum is $\Delta\lambda = 0.305$ nm, centered at 1568.4 nm with an average output power of 288.56 μW. Figure 6(c) shows the corresponding autocorrelation function, measured with a Femtochrome FR-103XL autocorrelator. The pulses were best fitted by a Sech^2 profile function, as indicated by the fitting curve. The pulse duration (T_{FWHM}) is measured as 8.8 ps from the FWHM time delay (T_{ac}) of 13.6 ps ($T_{FWHM} = 0.648\ T_{ac}$), and a maximum peak power of 6.0 W is estimated from the average power. These measurements together with the spectral bandwidth allow us to estimate the time-bandwidth product (TBP) as 0.325. By comparing this result with the transform-limit value of 0.315 for a Sech^2 pulse profile, it suggests that the pulses from our laser setup are very close to transform-limited. Figure 6(d) shows the RF spectrum of the output pulses, measured with a

3.2 GHz spectrum analyzer at the fundamental repetition frequency, using a 8 MHz span and 1 kHz resolution bandwidth. The frequency peak of the mode-locked pulses at 4.865 MHz is clearly observed along with two side frequency components at ± 2.435 MHz, indicating a small amplitude modulation imposed at the acoustic wave frequency. The signal to noise ratio (SNR) of the fundamental frequency peak was measured to be as high as 62 dB. The inset in figure 6(d) displays an extended view of the harmonic frequency signals in a frequency span of 50 MHz and 30 kHz resolution.
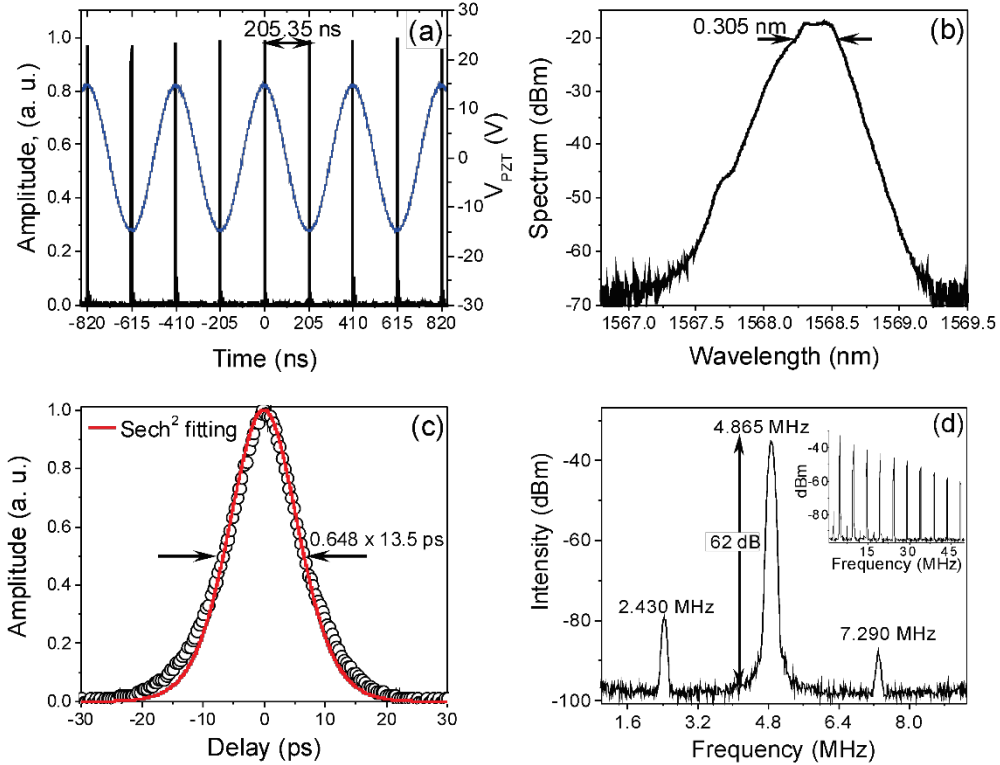

Figure 6. (a) Mode-locked train of pulses generated at 4.869735 MHz with 616 mW of pump power. (b) Measured optical spectrum of the laser. (c) Autocorrelation trace corresponding to output pulses. The red line indicates a Sech^2 profile fitting. (d) RF spectrum of the output pulse train measured with 8 MHz span and 1 kHz resolution bandwidth. The inset displays an extended RF spectrum with 50 MHz span and 30 kHz resolution.

A characterization of the pulses parameters in function of the pump power, RF voltage, frequency detuning and temporal stability is illustrated in figure 7. Mode-locking operation was found in a range between 602 and 616 mW of pump power. From figure 7(a), it can be observed an opposite behavior for the pulse width and peak power, the pulse width decreases whereas the peak power increases with the pump power. At the highest pump power, pulses as short as 8.8 ps were obtained with a peak power of 6.0 W. The dependence on the RF voltage is shown in figure 7(b), this dependence directly affects the strength of the acoustic wave, and consequently the modulation depth. For this measurement, the polarization adjustment and the acoustic frequency (4.869735 MHz) were maintained constant throughout the measurements process. The range of voltages to maintain mode-locking operation was found between 29.6 and 30.4 V. One can observe the narrowing of the output pulses as the voltage increases, from 10.5 ps at 29.6 V down to 8.75 ps at 30.4 V. According to AM mode-locking theory, the modulation depth and the pulse width are inverse parameters [21,22]. Hence, the pulse narrowing is an expected behavior. Another important parameter to quantify is the detuning in frequency (Δf_a), which determines the maximum allowable frequency drift with respect to the fundamental cavity frequency. Figure 7(c) shows the variation of the pulses parameters as the frequency of the RF signal is changed, similar to the previous

case, the polarization adjustment, V_{PD} (30.4 V) and pump power (616 mW) were kept constant. Mode locking of this laser permits a maximum detuning of about ± 6 Hz in any direction. This last result implies a maximum allowable cavity length drift (ΔL) no longer than ± 106 μm ($\partial L_{cavity}/\partial f_a = -17.6$ μm/Hz). Thus, high accuracy in frequency tuning is required. Figure 7(d) shows the temporal stability of the shortest optical pulse monitored for 1 hour on the autocorrelator. During this time the pulse width oscillates between 8.8 and 11.87 ps, with corresponding peak powers of 6.0 and 3.18 W, respectively. This last result demonstrates a relatively good stability for this kind of AO devices. However, a more stable operation could be possible by reducing the length of the modulator, which is the principal source of instability.
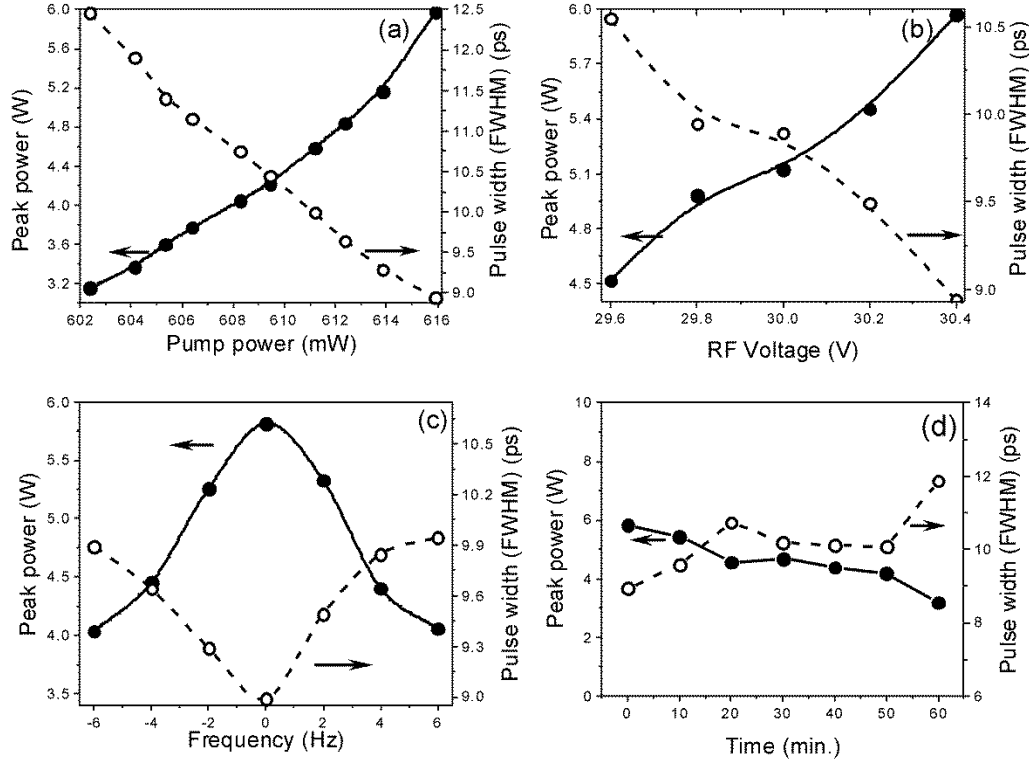

Figure 7. Dependence of the pulse width (FWHM) and peak power as a function of (a) pump power, (b) RF voltage and (c) frequency detuning. (d) Temporal stability of the shortest optical pulse monitored every 10 minutes for 1 hour. In all cases the solid points represent peak power and open points the pulse width.

If we compare the shortest optical pulse obtained with the present scheme (8.8 ps and 6.0 W of peak power) with the results obtained in [9], where optical pulses of 24 ps and 2.7 W of peak power were generated by using a similar AO modulator, but operating under a different configuration, there is an improvement by almost a factor of 3 for the pulse width and 221 % for the peak power. However, the main enhancement is produced by the modulator, which eliminates the need for additional filtering devices leading to a simplified mode-locking operation. One example of this versatility is shown in figure 8, where a tunable response is observed just by adjusting the cavity length with the acoustic wave frequency.
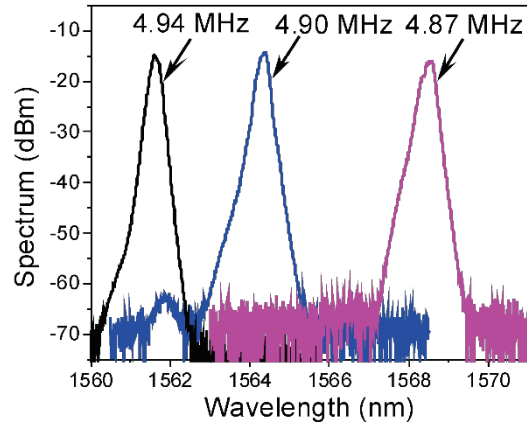
Figure 8. Tunable mode-locking operation of the fiber laser at different modulation frequencies. The arrows indicate the modulation frequency

The soliton number N of the shortest optical pulse, defined as the square root of the ratio between the dispersion and the nonlinear lengths, is estimated as 3.02 considering a dispersion value D of 20 ps/nm/km for the SMF-28 fiber. From this result, a pulse width reduction is probably enhanced by the creation of soliton pulses, as expected in the anomalous dispersion regime [23]. Furthermore, improvements in pulse width could be also possible by the inclusion of tapered optical fibers in the modulator. The gradual confinement of the acoustic wave into a reduced fiber diameter leads to a strong acousto-optic interaction, which results in a more efficient intermodal coupling [24,25]. In this way, improvements in optical bandwidth and interaction length of the modulator are feasible.

4. Conclusion

In this work we have carried out an experimental characterization of an actively mode-locked all-fiber ring laser by utilizing an in-fiber acousto-optic tunable bandpass modulator (AOTBM). The AOTBM modulator is based on a CMB, composed of a tiny section of coreless optical fiber (1.185 mm) spliced between two sections of standard single-mode fibers. First, we have presented a detailed characterization of the modulator itself. The AOTBM permits the implementation of relatively broad modulation bandwidth (1.4 nm), high modulation depth (74 %), and low optical loss (4.11 dB) in a 72.5-cm long configuration. Then, the effectiveness of the modulator is demonstrated by implementing active mode-locking operation. The modulator provides efficient spectral filtering to support ultrashort pulse generation. Transform-limited optical pulses of 8.8 ps temporal width and 6.0 W peak power were obtained at 4.869735 MHz repetition rate. These experimental results can be considered among the best results reported in the framework of actively mode-locked all-fiber lasers based on in-fiber AO modulators.

References
[1]   Diels J C and Rudolph 2006 *Ultrashort Laser Pulse Phenomena: Fundamentals, Techniques, and Applications on a Femtosecond Time Scale* (Academic press)
[2]   Nolte S, Schrempel F and Dausinger F 2016 *Ultrashort Pulse Laser Technology: Laser Sources and Applications* (Springer international publishing)

[3] Malmstrom M, Margulis W, Tarasenko O, Pasiskevicius V and Laurell F 2012 Soliton generation from an actively mode-locked fiber laser incorporating an electro-optic fiber modulator *Opt. Express* **20** 2905–10

[4] Nguyen D T, Abou J and Morimoto A 2012 Ultrashort pulse generation using fiber FM laser *Opt. Rev.* **19** 337–40

[5] Cuadrado Laborde C, Bello Jiménez M, Díez A, Cruz J L and Andrés M V 2012 Long-cavity all-fiber ring laser actively mode locked with an in-fiber bandpass acousto-optic modulator *Opt. Lett.* **39** 68–71

[6] Kim J, Koo J and Lee J H 2017 All-fiber acousto-optic modulator based on a cladding-etched optical fiber for active mode-locking *Photon. Res.* **5** 391–5

[7] Myren N and Margulis W 2005 All-Fiber Electrooptical Mode-Locking and Tuning *IEEE Phot. Tech. L.* **17**, 2047–9

[8] Yin K, Zhang B, Yang W, Chen H, Chen S and Hou J 2014 Flexible picosecond thulium-doped fiber laser using the active mode-locking technique *Opt. Lett.* **39** 4259–62

[9] Bello Jiménez M, Cuadrado Laborde C, Díez A, Cruz J L, Andrés M V and Rodríguez Cobos A 2013 Mode-locked all-fiber ring laser based on broad bandwidth in-fiber acousto-optic modulator *Appl. Phys.* B **110**, 73–80

[10] Bello Jiménez M, Cuadrado Laborde C, Sáez Rodríguez D, Díez A, Cruz J L and Andrés M V 2010 Actively mode-locked fiber ring laser by intermodal acousto-optic modulation *Opt. Lett.* **35** 3781–3

[11] Bello Jiménez M, Cuadrado Laborde C, Díez A, Cruz J L and Andrés M V 2011 Experimental study of an actively mode-locked fiber ring laser based on in-fiber amplitude modulation *Appl. Phys.* B **105**, 269–76

[12] Cuadrado Laborde C, Díez A, Delgado Pinar M, Cruz J L and Andrés M V 2009 Mode locking of an all-fiber laser by acousto-optic superlattice modulation *Opt. Lett.* **34**, 1111–3

[13] Cuadrado Laborde C, Díez A, Cruz J L and Andrés M V 2010 Experimental study of an all-fiber laser actively mode-locked by standing-wave acousto-optic modulation *Appl. Phys.* B **99**, 95–9

[14] Jeon M, Lee H K, Kim K H, Lee E, Oh W, Kim B Y, Lee H and Koh Y W 1998 Harmonically mode-locked fiber laser with an acousto-optic modulator in a Sagnac loop and Faraday rotating mirror cavity *Opt. Commun.* **149**, 312–6

[15] Culverhouse D O, Richardson D J, Birks T A and Russell P S J 1995 All-fiber sliding-frequency Er3+/Yb3+ soliton laser *Opt. Lett.* **20**, 2381–3

[16] Ramírez Meléndez G, Bello Jiménez M, Pottiez O and Andrés M V 2017 Improved all-fiber acousto-optic tunable bandpass filter *IEEE Phot. Tech. L.* **29**, 1015–8

[17] Ramírez Meléndez G, Bello Jiménez M, Pottiez O, Escalante-Zarate L, López Estopier R, Ibarra Escamilla B, Durán Sanchez M, Kuzin E A and Andrés M V 2017 Q-switching of an all-fiber ring laser based on in-fiber acousto-optic bandpass modulator *Appl. Phys.* B **123**, 249

[18] Alcusa Sáez E P, Díez A, Rivera Pérez E, Margulis W, Norin L and Andrés M V 2017 Acousto-optic interaction in polyimide coated optical fibers with flexural waves *Opt. Express* **25**, 17167–73

[19] Yeom D I, Kim H S, Kang M S, Park H S and Kim B Y 2005 Narrow-bandwidth all-fiber acoustooptic tunable filter with low polarization sensitivity *IEEE Photon. Technol. L.* **17** 2646–8

[20] Kim H S, Yun S H, Kwang I K and Kim B Y 1997 All-fiber acousto-optic tunable notch filter with electronically controlable spectral profile *Opt. Lett.* **22,** 1476–8

[21] Kuizenga D J and Siegman A E 1970 FM and AM mode locking of the homogeneous laser– part 1: theory *IEEE J. Quantum Elect.* **QE-6**, 694–708

[22] Li Y, Lou C, Han M and Gao Y 2001 Detuning characteristics of the AM mode-locked fiber laser *Opt. Quant. Electron.* **33**, 589–97

[23] Jones D J, Haus H A and Ippen E P 1996 Subpicosecond solitons in actively mode-locked fiber lasers *Opt. Lett.* **21**, 1818–20

[24] Li Q, Liu X, Peng J, Zhou B, Lyons E R and Lee H P 2002 Highly efficient acoustooptic tunable filter based on cladding etched single-mode fiber *IEEE Phot. Technol. L.* **14**, 337–9

[25] Abrishamian F, Nagai S, Sato S and Imai M 2008 Design theory and experiment of acousto-optical tunable filter by use of flexural waves applied to thin optical fiber *Opt. Quant. Electron.* **40**, 665–76